

# Control of the colossal magnetoresistance by strain effect in $\text{Nd}_{0.5}\text{Ca}_{0.5}\text{MnO}_3$ thin films.

E. Rauwel-Buzin<sup>1</sup>, W. Prellier<sup>1,\*</sup>, Ch. Simon<sup>1</sup>, S. Mercone<sup>1</sup>, B. Mercey<sup>1</sup>, B. Raveau<sup>1</sup>, J. Sebek<sup>2</sup> and J. Hejtmanek<sup>2</sup>

<sup>1</sup> *Laboratoire CRISMAT, CNRS UMR 6508, Bd du  
Maréchal Juin, 14050 Caen Cedex, FRANCE.*

<sup>2</sup> *Institute of Physics, Na Slovance 2, 182 21 PRAHA 8, Czech Republic.*

(April 26, 2024)

## Abstract

Thin films of  $\text{Nd}_{0.5}\text{Ca}_{0.5}\text{MnO}_3$  manganites with colossal magnetoresistance (CMR) properties have been synthesized by the Pulsed Laser Deposition technique on (100)- $\text{SrTiO}_3$ . The lattice parameters of these manganites and correlatively their CMR properties can be controlled by the substrate temperature  $T_S$ . The maximum CMR effect at 75K, calculated as the ratio  $\rho(H = 0T)/\rho(H = 7T)$  is  $10^4$  for a deposition temperature of  $T_S = 680^\circ\text{C}$ . Structural studies show that the  $\text{Nd}_{0.5}\text{Ca}_{0.5}\text{MnO}_3$  film is single phase, [010]-oriented and has a pseudocubic symmetry of the perovskite subcell with  $a = 3.77\text{\AA}$  at room temperature. We suggest that correlation between lattice parameters, CMR and substrate temperature  $T_S$  result mainly from substrate-induced strains which can weaken the charge-ordered state at low temperature.

---

\*prellier@ismra.fr

Numerous investigations of the manganites  $\text{Ln}_{1-x}\text{Ca}_x\text{MnO}_3$  (Ln=lanthanides) have been performed last years on bulk ceramics, showing that the colossal magnetoresistance (CMR) in these materials originates from a competition between metallic ferromagnetism (FM) and charge-ordered (CO) insulating antiferromagnetism (AFM)<sup>1,2</sup>. The magnetotransport properties of these compounds are sensitive to the sample nature- i.e. single crystal, ceramic, thin film; the studies of manganite thin films<sup>3-9</sup> and their properties being often different from the bulk ceramics or single crystals.

The great potentiality of thin films for device applications makes that their magnetotransport properties need to be investigated in detail in the future. In this respect, our recent studies of  $\text{Pr}_{0.5}\text{Ca}_{0.5}\text{MnO}_3$  thin films<sup>8,9</sup> have shown that the substrate-induced strains play a key role in the appearance of CMR by decreasing the stability of the charge-ordered (CO) state. Keeping in mind the key effect of the A-site cation size observed for bulk manganites<sup>10</sup>, it is of a great interest to extend previous studies to  $\text{Nd}_{0.5}\text{Ca}_{0.5}\text{MnO}_3$  (NCMO) thin films despite that unreasonably large magnetic field ( $>20$  T) were reported to melt the AFM charge ordered state below 200 K in bulk samples<sup>11</sup>. Moreover no direct confirmation of a complete conversion to FM metallic state was claimed.

In the present letter, we show that  $\text{Nd}_{0.5}\text{Ca}_{0.5}\text{MnO}_3$  thin films, grown on  $\text{SrTiO}_3$  by pulsed laser deposition (PLD), exhibit spectacular CMR effect at 7T, involving an insulator-to-metal transition around 100K. We demonstrate that the perovskite subcell at room temperature (RT) varies with the temperature of the substrate during deposition, and correlatively, the CMR effect is controlled by the growth conditions. The correlations between CMR and lattice parameters are interpreted in terms of strains effects due to the substrate and oxygen non-stoichiometry.

Dense targets of  $\text{Nd}_{0.5}\text{Ca}_{0.5}\text{MnO}_3$  were synthesized via the standard ceramic methods. The PLD apparatus has been described in detail elsewhere<sup>8,9</sup>. Briefly, an excimer laser (Lambda Physics, with a  $\lambda = 248\text{nm}$  pulse rate of  $3\text{Hz}$ , was focussed onto a rotating target.  $1200\text{\AA}$  thick films were deposited on (100)- $\text{SrTiO}_3$  (STO) substrates heated during deposition at constant temperature ranging from  $590^\circ\text{C}$  to  $770^\circ\text{C}$  under an oxygen pressure

of about 300mTorr. Details of the growth parameters will be discussed hereafter. Structural characterizations were done using an X-ray diffraction (XRD) facility (Seifert 3000 P for  $\Theta$ - $2\Theta$  and Philips X'Pert MRD for in-plane measurements, Cu  $K\alpha$  with  $\lambda = 1.5406\text{\AA}$ ). Resistivity ( $\rho$ ) of NCMO films was measured with a PPMS Quantum Design as a function of magnetic field ( $H$ ) and temperature ( $T$ ) using 4-probe contact. The Energy Dispersive Spectroscopy analyses have shown that the cationic composition the film is homogeneous and remains very close to the nominal one "Nd<sub>0.5±0.02</sub>Ca<sub>0.5±0.02</sub>MnO<sub>x</sub>" within experimental error.

In order to obtain simultaneously as good crystallization and full oxidized films, we have performed the synthesis under 400mtorr of O<sub>2</sub> since the preparation of manganites with high Mn valency usually require a high oxygen pressure, or a post-annealed treatment<sup>12</sup>. The best results concerning CMR were obtained for a substrate temperature ( $T_S$ ) of 680°C and, consequently, following study was focused on this sample. The corresponding XRD patterns confirm a single phase (Fig. 1) with an out-of-plane parameter multiple of  $a_C$  (where  $a_C$  refers to the ideal cubic parameter 3.9Å). The high intensity of the peak indicating a good crystallization for the film is independently confirmed by the full-width-at half maximum of the rocking-curve equal to 0.25°(not shown). The sharp peaks 90°-separated in the  $\Phi$ -scan of the NCMO film (see inset of Fig. 1) make evident the existence of a complete in-plane orientation of the film. In a sake of clarity the diffraction peak around  $2\Theta = 47^\circ$  (see Fig.1) has been indexed in the perovskite cell as a  $(002)_C$  (where  $c$  refers to the cubic perovskite cell). In fact, the electron diffraction study of selected NCMO films confirmed that they are single phase. We have found that they are [010]-oriented referring to the  $Pnma$  space group<sup>13</sup> as previously reported for Pr<sub>0.5</sub>Ca<sub>0.5</sub>MnO<sub>3</sub> thin films grown on (100)-SrTiO<sub>3</sub> substrates<sup>8</sup>. The details of the transmission electron microscopy study are currently undertaken and will be published elsewhere. The in-plane parameter has been evaluated by considering the  $(103)_C$  reflection; It is remarkable that the parameters of the perovskite subcell are very close to each other, i.e. 3.775Å and 3.765Å for the in-plane and out of plane parameters respectively. This indicates a pseudo cubic symmetry which is similar to the bulk Nd<sub>0.5</sub>Ca<sub>0.5</sub>MnO<sub>3</sub>, but

the latter exhibits significantly larger cell parameters at RT ( $a/\sqrt{2} = 3.821\text{\AA}$ ,  $b/2 = 3.797\text{\AA}$  and  $c/\sqrt{2} = 3.805\text{\AA}$ <sup>13</sup>). But as more important we emphasize the substantial variation of RT lattice parameters with the deposition temperature  $T_S$ , in the range  $620^\circ\text{C}$  to  $780^\circ\text{C}$ . This dependence is shown in Figure 2a. Indeed for  $T_S$  ranging from  $620^\circ\text{C}$  to  $680^\circ\text{C}$  the symmetry remains pseudocubic and the cell parameters decrease almost linearly with increasing  $T_S$ . Contrary to that for  $T_S > 680^\circ\text{C}$ , a sudden distortion of the perovskite subcell appears, the in plane and out of plane parameters being very different, and further increase with  $T_S$ . From this observations we deduce that the strains induced by the substrate are not the only factor which governs the crystallographic nature of the film and we presume that the oxygen stoichiometry of NCMO thin film varies with the deposition temperature. This general statement is reinforced by the evolution of the cell volume versus  $T_S$  (Fig. 2a) when below  $680^\circ\text{C}$  the volume decrease likely suggests an oxygen uptake with increasing  $T_S$  due to increasing Mn valency ( $\text{Mn}^{4+}$  for  $\text{Mn}^{3+}$  substitution), whereas above  $680^\circ\text{C}$  the volume increase can be explained by an oxygen departure -i.e.  $\text{Mn}^{3+}$  for  $\text{Mn}^{4+}$  substitution.

Keeping in mind that the substrate-induced strains may crucially affect the temperature and stability of phase transitions, we may expect that the CMR properties of films will depend upon the crystallographic nature of the room temperature form and, consequently, upon the deposition temperature  $T_S$ . We have focussed our study on the best crystallized films deposited under 400mtorr of  $\text{O}_2$  in the temperature range of  $620^\circ\text{C}$  and  $680^\circ\text{C}$  (below  $620^\circ\text{C}$ , the crystallization of the film is poor). As stated above, the best result was observed for the film grown at  $680^\circ\text{C}$ . The  $\rho(T)$  curve registered in absence of magnetic field and at 7T are shown in Fig.3a first order insulator to metal transitions, characterized by a hysteretic resistivity jump of several orders of magnitude (see also  $\rho(H)$  in the inset Fig.3a). According to our knowledge such a sharp transition has never been detected before in thin films. In context to the metallic ground state at low temperatures, let us underline the very low value of residual resistivity ( $\sim 30\text{m}\Omega\text{cm}$ ) which independently confirms both the high quality of the film and the complete transformation to FM metallic phase.

Thus based on resistivity measurements we deduce a phase diagram- see Fig.3b. Using the hysteresis cycles in the field ramping up ( $H_C^+$ ) and ramping down ( $H_C^-$ ), we define the thermodynamic field ( $H_C$ ) as the average of ( $H_C^+$ ) and ( $H_C^-$ ). In Fig. 3b,  $H_C$  shows a monotonous increase with temperature when  $T < 150\text{K}$ .  $H_C$  is estimated to be 3T at 25 K, which is 6-7 times lower than the 25T found in the bulk material with the same chemical composition<sup>11</sup>. In fact, our phase diagram of 680°C deposited NCMO film is very different from the bulk where the magnetic field required to melt the charge ordered state is much higher at each temperature<sup>11</sup>.

The second important point of the paper concerns the influence of the deposition temperature  $T_S$  of NCMO films up on the CMR effect. The evolution of the resistance ratio  $RR = \rho(H = 0T)/\rho(H = 7T)$  vs.  $T_S$  (Fig.2b) shows that the  $RR$  increases as  $T_S$  increases up to  $T_S = 680^\circ\text{C}$  and suddenly decreases for  $T_S > 680^\circ\text{C}$ . It is straightforward to correlate this evolution to the lattice parameters :

- the CMR effect increases in the pseudocubic region as the lattice parameters at room temperature decrease reaching a maximum value of  $10^4$  for a minimum average lattice parameter of  $3.77\text{\AA}$  (corresponding to  $T_S = 680^\circ\text{C}$ )

- then it drops abruptly in the distorted lattice region as the parameters increase. Similar evolutions are observed for  $RR$  measured at  $T = 100\text{K}$  and  $125\text{K}$ , while the maximum  $RR$  value rapidly decreases, as one approaches  $T_{CO}$  ( $T_{CO}=250\text{ K}$ ).

The dramatic influence of the substrate temperature  $T_S$  upon both, lattice parameters and CMR properties of  $Nd_{0.5}Ca_{0.5}MnO_3$  thin films suggests that two factors influence their properties , the oxygen stoichiometry and the strains induced by the substrate. Concerning the influence of the oxygen stoichiometry, the study on bulk ceramics by Frontera et al.<sup>14</sup> has shown, that an oxygen overstoichiometry in  $Nd_{0.5}Ca_{0.5}MnO_{3+\delta}$  leads to a significant variation of the structural and magnetic properties, namely the formally excess oxygen induces the increase of ferromagnetic interactions at low temperatures. Nevertheless, the lattice and CMR effects encountered for our NCMO films are huge compared to the  $Nd_{0.5}Ca_{0.5}MnO_{3+\delta}$  ceramics, so we do not suppose that oxygen non-stoichiometry is the

only factor controlling the properties of our films. The second factor dealing with the strains induced by the substrate, previously observed for other CO manganites<sup>8,9,15</sup>, has at least the same prominence since, as previously observed, the substrate-layer strain is susceptible e.g. weakening the CO state, by blocking the variation of the in-plane lattice parameters with increasing temperature<sup>9</sup>, thus favoring the CMR effect.

To conclude, high quality  $\text{Nd}_{0.5}\text{Ca}_{0.5}\text{MnO}_3$  thin films, with exceptional CMR properties have been grown using pulsed laser deposition. The room temperature lattice parameters and their CMR properties of films are correlated and can be controlled by the deposition temperature  $T_S$ . We suggest that observed correlations between structural and transport properties in NCMO films result predominantly from substrate-induced strains which can destabilize the charge-ordered state.

Acknowledgements: W. Prellier thanks Dr C. Frontera for helpful discussions.

## REFERENCES

- <sup>1</sup> Colossal Magnetoresistance oxides, Edit. Y. Tokura, Gordon and Breach, London 1999.
- <sup>2</sup> Colossal Magnetoresistance, Charge ordering and Related Properties of Manganese oxides, Edit. C.N.R. Rao and B. Raveau, World Scientific, Singapore, 1998.
- <sup>3</sup> T. Venkatesan, M. Rajeswari, Z-W. Dong, S.B. Ogale and R. Ramesh, Phil. Trans. R. Soc. London 356, 1661 (1998).
- <sup>4</sup> R. Von Helmolt, J. Wecker, R. Holzapfel, L. Schultz, K. Samwer, Phys. Rev. Lett. 71, 2331 (1993).
- <sup>5</sup> H.L. Ju, C. Kwon, Q. Li, R.L. Greene and T. Venkatesan, App. Phys. Lett. 65, 2108 (1994).
- <sup>6</sup> S. Jin, T.H. Tiefel, M. Mc Cormack, R.A. Fastnacht, R. Ramesh and L.H. Chen, Science 264, 413 (1994).
- <sup>7</sup> G.C. Xiong, Q. Li, H.L. Mao, S.N. Senapati, X.X. Xi, R.L. Greene and T. Venkatesan, App. Phys. Lett. 66, 1427 (1995).
- <sup>8</sup> W. Prellier, A.M. Haghiri-Gosnet, B. Mercey, Ph. Lecoœur, M. Hervieu and B. Raveau, App. Phys Lett. 77, 1023 (2000), W. Prellier, Ch. Simon, A.M. Haghiri-Gosnet, B. Mercey and B. Raveau, Phys. Rev. B 62, 16337 (2000).
- <sup>9</sup> A.M. Haghiri-Gosnet, M. Hervieu, Ch. Simon, B. Mercey and B. Raveau, J. App. Phys. 88, 3545 (2000).
- <sup>10</sup> A. Sundaresan, A. Maignan and B. Raveau, Phys. Rev. B 56, 5092 (1997), F. Millange, A. Maignan, V. Caignert, Ch. Simon and B. Raveau, Z. für Physik B 101, 169 (1996).
- <sup>11</sup> M. Tokunaga, N. Miura, Y. Tomioka, Y. Tokura, Phys. Rev. B. 57, 5259 (1998).
- <sup>12</sup> W. Prellier, A. Biswas, M. Rajeswari, T. Venkatesan and R.L. Greene, App. Phys. Lett. 75, 397 (1999).

<sup>13</sup> F. Millange, S. de Brion and G. Chouteau, Phys Rev. B 62, 5619 (2000).

<sup>14</sup> C. Frontera and J.G. Garcia-Munoz, A. Llobet, C. Ritter, J.A. Alonso, J. Rodriguez-Carvajal, Phys. Rev. B 62, 3002 (2000).

<sup>15</sup> B. Mercey, M. Hervieu, W. Prellier, J. Wolfman, Ch. Simon and B. Raveau, submitted to App. Phys. Lett. (2001).

Figures Captions:

Fig.1: Room temperature  $\Theta$ - $2\Theta$  XRD pattern in the range  $35$ - $50^\circ$  of NCMO/STO. The inset depicts the  $\Phi$ -scan recorded around the  $\{103\}_C$ .

Fig.2a: Evolution of the lattice parameters and the volume of the cell vs. deposition temperature for films grown under 400mTorr of  $O_2$ .

Fig.2b: CMR effect calculated as  $\rho(H = 0)/\rho(H = 7T)$  vs. the deposition temperature (400mTorr of  $O_2$  was used).

Fig.3a:  $\rho(T)$  under different applied magnetic fields for an optimized film ( $T_S = 680^\circ C$ ). The inset shows the  $\rho(H)$  at 75K. Note the sharp transition and the CMR effect of 11 orders of magnitude at 7T. Field is applied parallel to the substrate plane. The arrows indicate the increase and the decrease in T.

Fig.3b: Corresponding  $T - H$  phase diagram. The dashed area indicates the hysteresis region where CO and FM phases coexist.

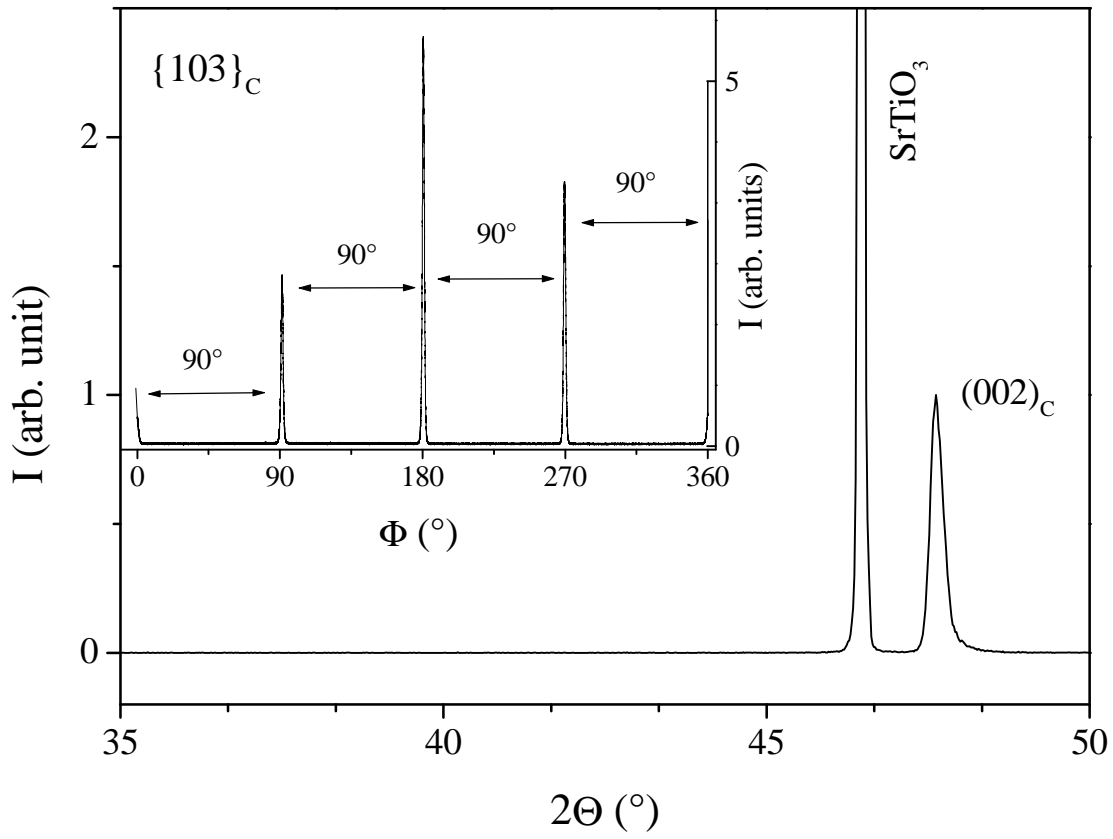


Figure 1

*E. Rauwel-Buzin et al.*



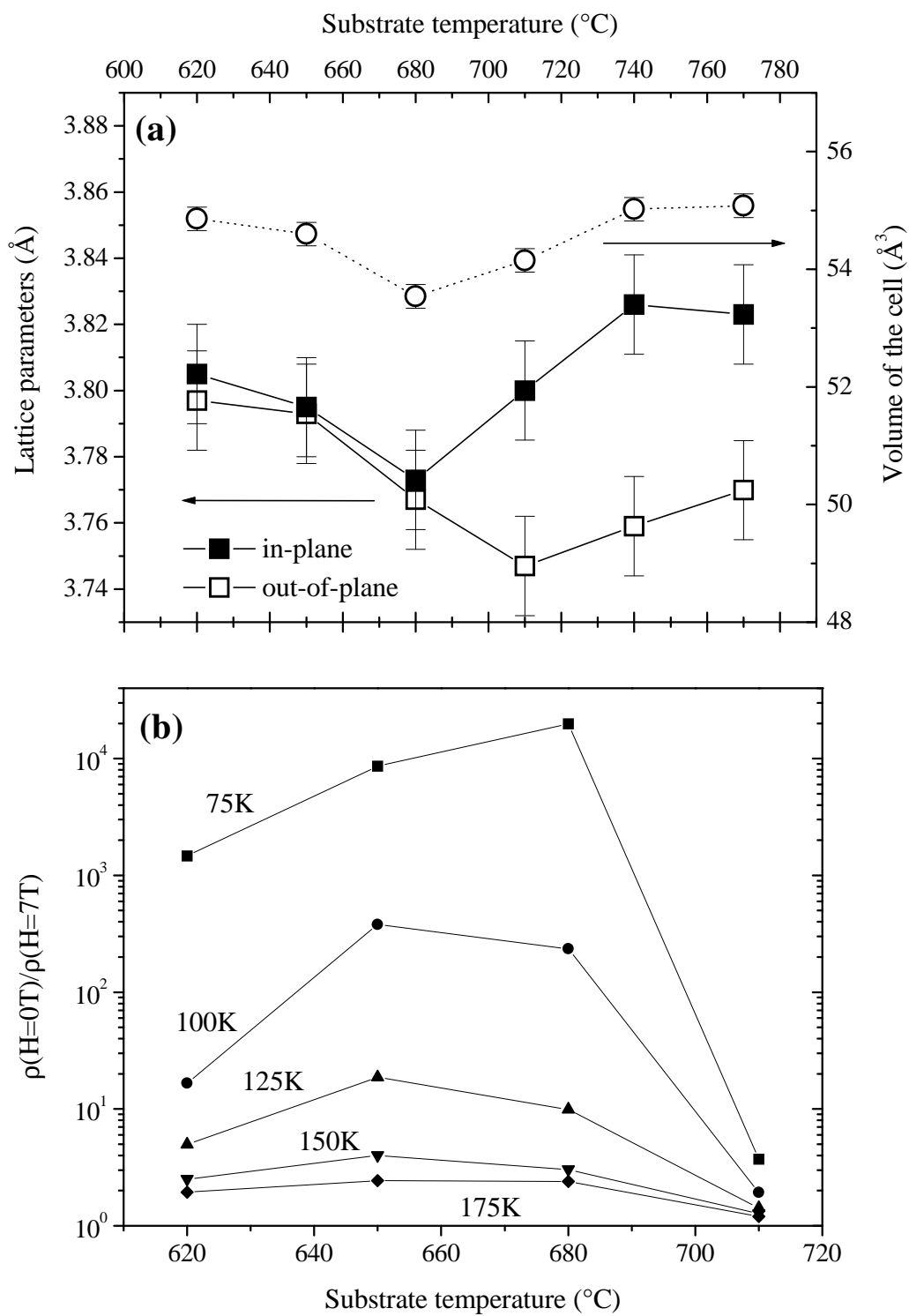


Figure 2

*E. Rauwel-Buzin et al.*



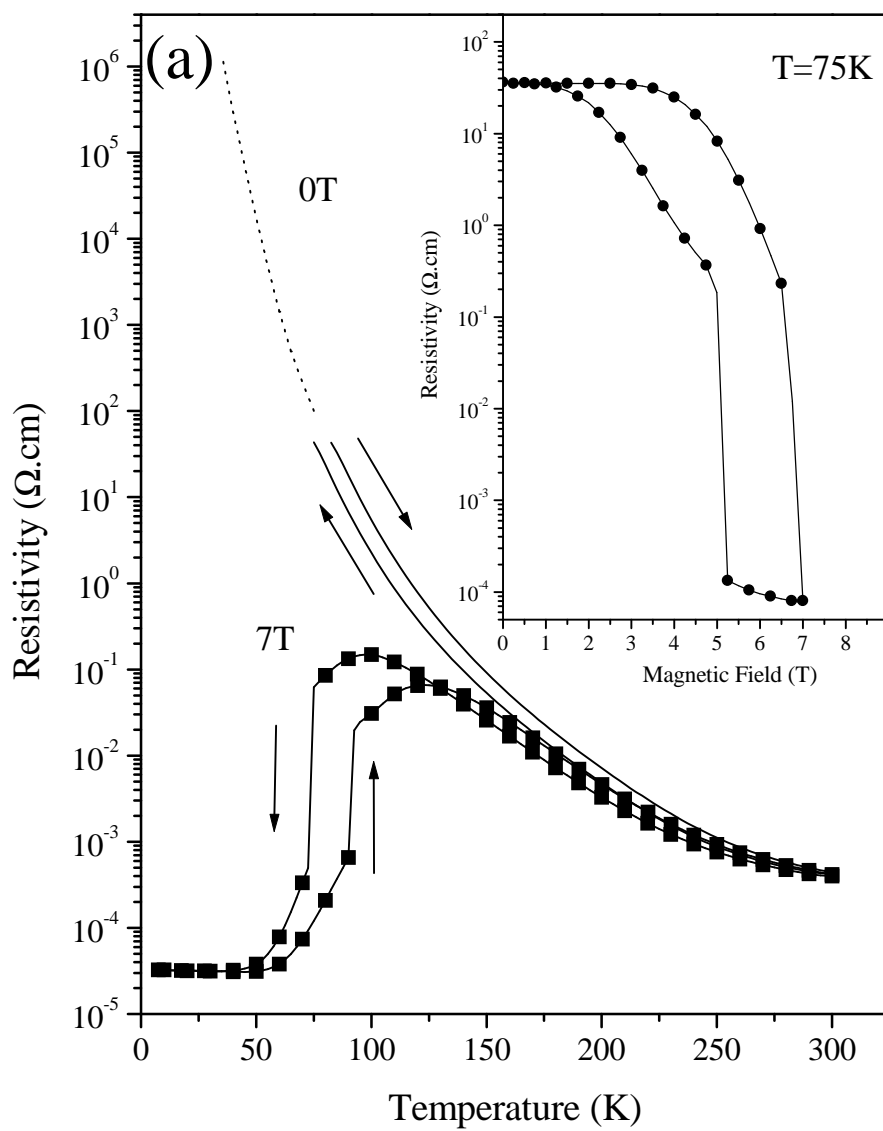


Figure 3a

*E. Rauwel-Buzin et al.*



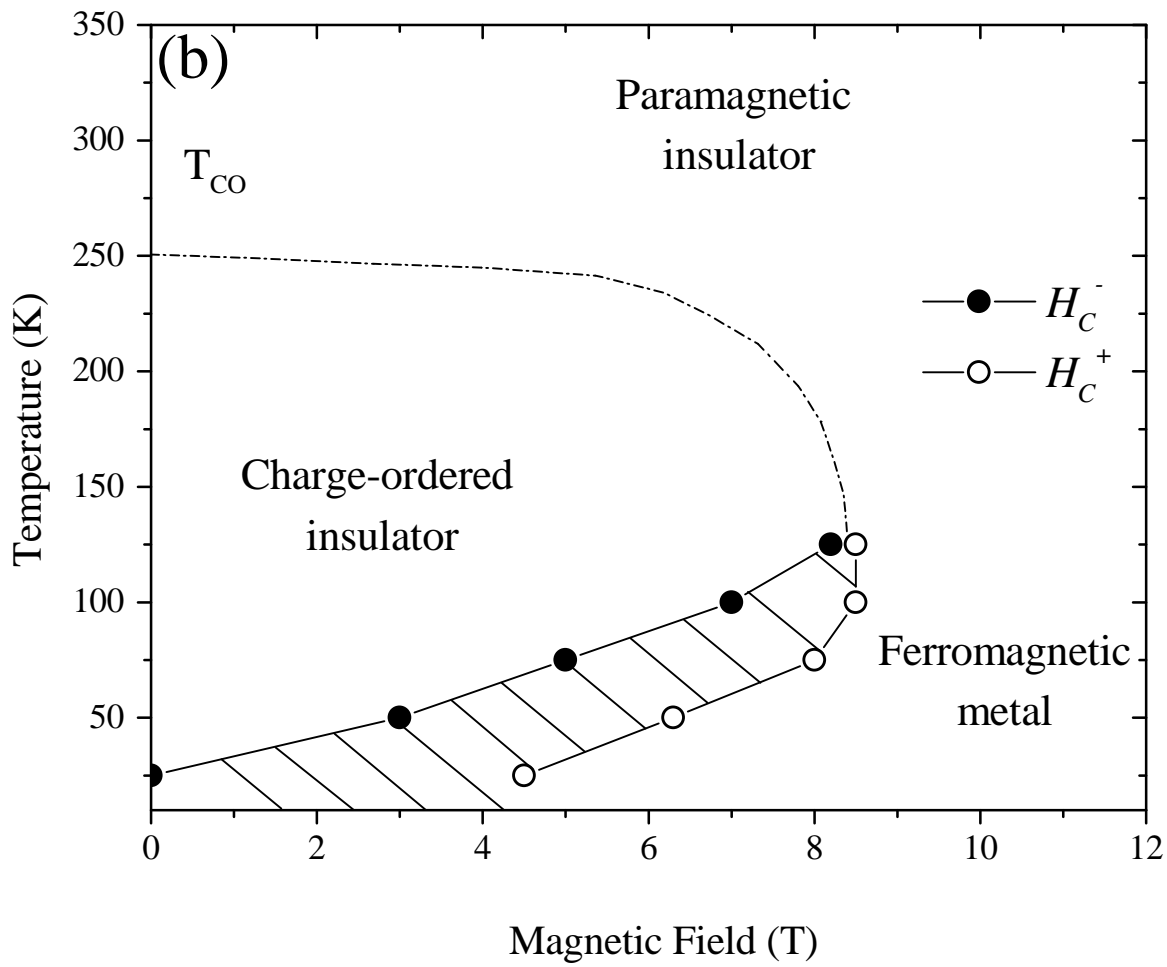


Figure 3b

*E. Rauwel-Buzin et al.*

